JOURNAL OF CATALYSIS 98, 178–190 (1986)

Platinum–Rhodium Synergism in Three-Way Automotive Catalysts

SE H. OH AND JOYCE E. CARPENTER

Physical Chemistry Department, General Motors Research Laboratories, Warren, Michigan 48090

Received April 24, 1985; revised October 4, 1985

The interactions between Pt and Rh in three-way automotive catalysts were investigated by conducting laboratory reactor experiments with both a Pt/Rh bimetallic catalyst (prepared by stepwise metal impregnation) and a physical mixture of Pt and Rh monometallic catalysts while holding the absolute amount of each of the noble metals constant. Activity measurements in a CO–NO–O_2 feedstream have shown that the CO oxidation activity of the bimetallic catalyst is substantially higher than that of the physical mixture over the concentration and temperature ranges characteristic of the converter warmup period. This synergistic enhancement of CO oxidation activity in the bimetallic catalyst can be rationalized by visualizing the catalyst surface structure as a statistical mixture of Pt and Rh sites. It was found that such a desirable surface structure (and the attendant synergistic activity enhancement) cannot be obtained by simultaneous impregnation of the noble metals because this catalyst preparation procedure leads to preferential Rh enrichment on the catalyst surface under the net-oxidizing reaction conditions considered in this study.

INTRODUCTION

Supported bimetallic catalysts often exhibit certain desirable properties (e.g., improved activity, selectivity, thermal stability, or poison resistance) which are absent in each of the individual metals. Much of the earlier work on bimetallic catalysts has been devoted to hydrocarbon reactions relevant to petroleum refining; two notable examples in this category are platinum/rhenium (*1–4*) and platinum/iridium (*4–6*) reforming catalysts.

Another bimetallic catalyst system of industrial importance is three-way catalysts used for the simultaneous conversion of carbon monoxide, hydrocarbons, and nitrogen oxides in automobile exhaust. Typical commercial three-way catalysts contain both platinum and rhodium, and electron microprobe examination of their cross section reveals that these two noble metals are located more or less in the same band. Despite the widespread use of three-way catalysts, little is known about the interaction between the metallic components.

In this paper we have investigated the activity of an alumina-supported Pt/Rh bimetallic catalyst in a laboratory CO–NO–O_2 feedstream. The nature and extent of Pt–Rh interactions in the bimetallic catalyst were ascertained by comparing its catalytic properties with those of a physical mixture of Pt and Rh monometallic catalysts while holding the absolute amount of each of the noble metals constant. Of particular interest here is the CO oxidation activity under conditions characteristic of the converter warmup period (i.e., relatively low temperatures and net-oxidizing gaseous environment).

EXPERIMENTAL

Catalysts. The three catalysts used in the experiments (Pt, Rh, and Pt/Rh) were all prepared by impregnating a low-density θ-alumina support (3.5-mm-diameter spheres, BET surface area = 116 m^2/g, pellet density = 0.761 g/cm^3) with a solution of the appropriate metal salt. The noble metal salts and techniques used in the impregnation, and the properties of the finished catalysts are

0021-9517/86 $3.00

TABLE 1

Preparation Methods and Characteristics of the Catalysts

	Pt	Rh	Pt/Rh
Metal salts	$H_2PtCl_6 \cdot 6H_2O$	$RhCl_3 \cdot 3H_2O$	$H_2PtCl_6 \cdot 6H_2O$ $RhCl_3 \cdot 3H_2O$
Impregnation technique	Acetone	Aqueous	Aqueous (Rh), then acetone (Pt)
Metal loading (wt%)	0.054	0.026	0.049 Pt, 0.023 Rh
CO uptake (μmol/g)[a]	1.6	2.3	3.5
CO/metal atom	0.59	0.90	0.74
Metal bandwidth (μm)[b]	36	27	33 Pt, 27 Rh

[a] Static CO chemisorption measurements over the fresh catalysts.

[b] Peak width at half-height of electron microprobe traces.

listed in Table 1. The conventional aqueous procedure was used for placement of the Rh band, while the Pt was deposited using a nonaqueous preparation method developed by D'Aniello (*7*). The latter method, which employs acetone as the impregnating solvent, generally yields metal bandwidths narrower than those obtained by established aqueous procedures. A detailed description of the acetone-based preparative procedure can be found in Ref. (*7*). Such procedures resulted in surface metal bands of similar widths (30 μm or so) for both the Pt and Rh catalysts. The bimetallic catalyst was prepared using a two-step impregnation procedure (aqueous impregnation of Rh followed by nonaqueous impregnation of Pt), with air-drying (room temperature, overnight) and calcination (300°C, 2 h) steps between successive noble metal impregnations. Following final impregnation, all the catalysts were dried in air overnight at room temperature and then calcined in air at 500°C for 4 h.

The dispersion of the Pt catalyst is calculated to be 59% based on the well-established 1:1 stoichiometry between Pt surface atoms and adsorbed CO molecules (see Table 1). The adsorption characteristics of CO on Rh are complex and dependent on such factors as metal loading (*8*), support (*9*), rhodium precursor (*10*), and postimpregnation heat treatment conditions (*11*). In general, low-loaded alumina-supported Rh catalysts, such as ours, give CO/Rh chemisorption ratios in excess of unity. The Rh dispersion of our catalyst is estimated to be 60% on the basis of a CO/Rh adsorption ratio of 1.5 reported previously (*12*) for low-loaded Rh/Al_2O_3 catalysts prepared and calcined using the same procedures as described here. This CO chemisorption stoichiometry is in general agreement with the infrared observations of both $Rh(CO)_2$ and RhCO species (*13*), indicating the presence of a mixture of isolated Rh atoms and small Rh clusters on the catalyst surface (*14*).

To investigate the effects of catalyst poisoning, all three catalysts were exposed to exhaust from a dynamometer-mounted 5.0-liter V-8 engine (EGR, 1800 rpm, 47-kPa manifold vacuum) operating on fuel doped with phosphorus (0.016 g P/liter added as tricresyl phosphate). During the poisoning, the air–fuel ratio was cycled ±0.5 unit about the stoichiometric point at 0.05 Hz. The use of a reactor equipped with compartmentalized screen trays (*15*) allowed simultaneous poisoning of all the catalysts. The reactor inlet temperature was maintained at approximately 450°C. (This relatively low poisoning temperature was chosen in order to minimize interference from sintering.) The catalysts were poisoned for a total of 35 h, and after every 5 h of poisoning the catalyst pellets were mixed thoroughly in an attempt to ensure a uniform poison distribution within each compartment. Electron microprobe observations of the pellet's cross section revealed that after the poisoning process, the entire noble metal band had been penetrated by P for all three catalysts considered. (The poison penetration depths for the Pt, Rh, and Pt/Rh catalysts were 44, 44, and 47 μm, respectively.)

The independent effect of high-temperature exposure was examined by thermally aging the catalysts for 40 h under three different conditions: (1) cycled exhaust at 700°C, (2) flowing air at 700°C, and (3) flowing air at 850°C. For the thermal aging in exhaust, the engine was operated at 2400 rpm and 44-kPa manifold vacuum, and the air–fuel ratio was cycled ±0.5 unit about the stoichiometric point at 0.05 Hz. Indolene clear fuel was used to minimize the accumulation of contaminants (P or Pb) in the catalysts.

Oxidation activity measurements. During the converter warmup period, three-way catalysts are usually operated in a net-oxidizing environment to oxidize CO and hydrocarbons in automobile exhaust. The oxidation activity of the catalysts was measured in laboratory CO–NO–O_2 feedstreams (in a N_2 background) using an internal-recycle mixed-flow reactor manufactured by the Autoclave Engineers (*16*). [We included NO in the feedstream because the CO oxidation rate over noble metals has been shown to be inhibited by NO (*17*)].

Catalytic activity was characterized in two ways—with fixed feed composition and with fixed outlet composition (variable temperature in both cases). Constant feed composition experiments involved monitoring steady-state outlet concentrations as a function of temperature (increased from room temperature to 450°C) in a feedstream of fixed composition. All the activity data reported here were obtained in the presence of excess oxygen at an impeller speed of 1500 rpm and a total feedstream flow rate of 5 liters/min (STP). The effects of CO and O_2 concentrations on the oxidation activity of the catalysts were examined by repeating the temperature runup experiments over a range of feedstream compositions (1 to 4.4 vol% CO, 1 to 11 vol% O_2, and 500 ppm NO). In reporting the data, we chose the temperature required to achieve 50% CO conversion as a direct measure of the oxidation activity of the catalysts; typical precision associated with this measurement is ±2°C of the reported value. In another series of activity measurements, the rate of CO oxidation was measured as a function of temperature while holding the reactant composition at the reactor outlet constant. Such constant outlet composition experiments with a CSTR such as our reactor allow one to directly compare the reaction rates over different catalysts under identical reaction conditions (i.e., same catalyst temperature and reactant composition).

RESULTS

Oxidation Activity: Pt vs Rh

Before discussing the behavior of the Pt/Rh bimetallic catalyst, it is instructive to examine the properties of the individual monometallic catalysts. One convenient measure of the oxidation activity of the catalysts during the converter warmup period is the temperature required to achieve 50% CO conversion in a net-oxidizing feedstream of fixed composition. Figure 1 shows how the 50% CO conversion temperature is affected by the CO concentration in the feed for the fresh 0.054 wt% Pt/Al_2O_3 and 0.026 wt% Rh/Al_2O_3 catalysts. The feedstream concentrations of O_2 (5 vol%) and NO (500 ppm) were held constant. For these experiments, the amounts of the catalysts (6.4 g of Pt/Al_2O_3 or 7.0 g of Rh/Al_2O_3) were chosen so that both samples contained essentially the same number of noble metal atoms. Thus, the results shown in Fig. 1 reflect the *specific* activity (i.e., activity per metal atom) of Pt and Rh for CO oxidation under net-oxidizing conditions. The observation that the temperature for 50% CO conversion for Pt increases mono-

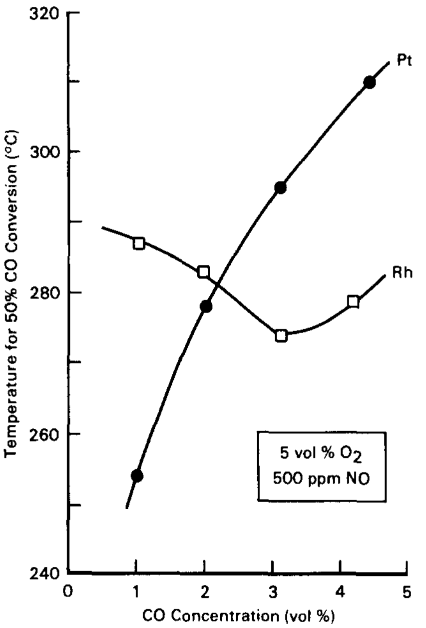

FIG. 1. Temperature for 50% CO conversion for the fresh Pt and Rh catalysts as a function of CO concentration in the feed. The numbers of noble metal atoms are the same in both cases.

tonically with increasing CO concentration in the feed is not surprising in view of the well-known inhibition of the CO oxidation rate by CO. Rh exhibits a similar but milder CO inhibition effect at high CO concentrations (>3 vol%). In the regime of lower CO concentrations (<3 vol%), the opposite trend was observed; that is, increasing CO concentration improves the CO oxidation activity (as evidenced by the decrease in the 50% conversion temperature), presumably by promoting the reduction of the otherwise oxide-covered inactive rhodium surface (*18, 19*).

Under the experimental conditions of Fig. 1 and subsequent figures (a large excess of CO over NO in the feed and relatively low NO conversion), the amount of CO consumed by the CO–NO reaction accounts for only a small fraction of the total amount of CO converted. Thus, the 50% CO conversion temperature observed during the temperature runup experiments can be viewed as a direct measure of the CO oxidation activity.

We also conducted temperature runup experiments as a function of inlet O_2 concentration (with the inlet concentrations of CO and NO fixed at 2 vol% and 500 ppm, respectively) using the same Pt and Rh samples. Figure 2 shows the results of such experiments. (The curve for Pt/Rh will be explained later.) In accord with our anticipation, the 50% CO conversion temperature for Pt decreases with increasing O_2 concentration. Interestingly, the Rh/Al_2O_3 catalyst exhibited the highest CO oxidation activity at an intermediate O_2 concentration (~8 vol%). This observation is consistent with the results of earlier kinetic measurements over Rh/Al_2O_3 (19). The increase in the 50% conversion temperature of the Rh/Al_2O_3 catalyst at higher O_2 concentrations (>8 vol%) can be explained by the formation of a relatively inactive Rh oxide under the strongly oxidizing conditions (18, 19).

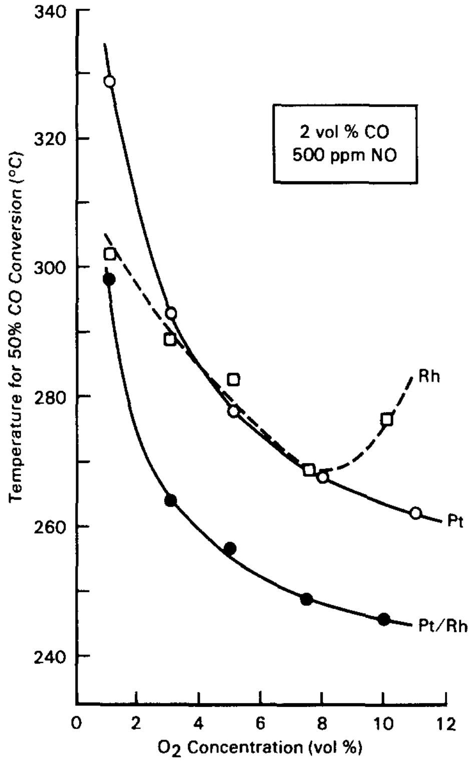

FIG. 2. Temperature for 50% CO conversion for the fresh Pt, Rh, and Pt/Rh catalysts as a function of O_2 concentration in the feed.

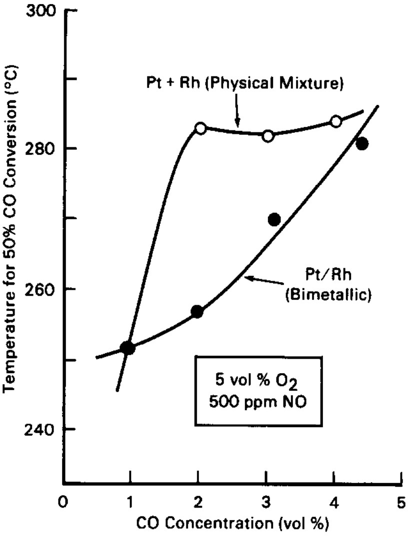

FIG. 3. Temperature for 50% CO conversion for the fresh bimetallic catalyst and physical mixture as a function of CO concentration in the feed. The absolute amounts of each of the noble metals are the same in both cases (53 at.% Pt).

It is evident from Figs. 1 and 2 that the relative activity of Pt and Rh changes with operating conditions. In general, Pt is more active for CO oxidation than Rh under strongly oxidizing conditions (low CO or high O_2 concentrations), while the reverse is true at high CO or low O_2 concentrations.

Oxidation Activity: Pt–Rh Synergism

As mentioned earlier, CO oxidation activity over a combination of Pt and Rh is an important part of three-way automotive emission control. Two different cases are considered here: a physical mixture of the Pt and Rh monometallic catalysts (Pt + Rh) and the bimetallic catalyst prepared by impregnating both Pt and Rh onto the same pellet (Pt/Rh). Figure 3 shows the 50% CO conversion temperature as a function of inlet CO concentration for the physical mixture (3.4 g of the 0.054 wt% Pt/Al_2O_3 catalyst + 3.3 g of the 0.026 wt% Rh/Al_2O_3 catalyst) and bimetallic catalyst (3.7 g of catalyst pellets containing 0.049 wt% Pt and 0.023 wt% Rh in the same band). The results for the physical mixture are consistent with what one would expect from the data for the individual metals shown in Fig. 1. The experimental data for the bimetallic catalyst, on the other hand, are somewhat surprising; the 50% CO conversion temperature for the bimetallic catalyst is considerably lower than that for the physical mixture (i.e., higher activity for the bimetallic catalyst) over the CO concentration range of 1 to 4%, despite the fact that they both contain the same absolute amount of each of the noble metals. This comparison clearly demonstrates that the coexistence of Pt and Rh in the same band of the pellet provides a synergistic enhancement of CO oxidation activity.

The results of Fig. 2 suggest that this Pt–Rh synergism also prevails in a plot of 50% conversion temperature vs O_2 concentration (with CO concentration held constant). Although not directly measured, the 50% CO conversion temperatures for the physical mixture of the Pt and Rh catalysts are expected to lie between those for the Pt and Rh catalysts. Comparison of these expected values with the experimental data for the Pt/Rh bimetallic catalyst indicates that the Pt–Rh synergism in the bimetallic catalyst leads to significant enhancement of CO oxidation activity over the wide range of O_2 concentrations of interest in converter warmup.

We conducted some experiments to investigate how the extent of the synergistic effect depends on the composition of the bimetallic catalyst. For these experiments, bimetallic catalysts with various Pt-to-Rh ratios were prepared by impregnating different amounts of Pt (using the acetone technique) onto the 0.026% wt% Rh/Al_2O_3 catalyst. Figure 4 shows the temperature for 50% CO conversion as a function of the atomic percentage (at. %) of Pt (with the total number of noble metal atoms in the catalyst sample held constant) for a feedstream containing 2 vol% CO, 5 vol% O_2, and 500 ppm NO. This particular feedstream composition was chosen because both Pt and Rh showed very similar 50%

TABLE 2

Temperatures for 50% CO Conversion in a 1% CO–5% O_2–500 ppm NO Feedstream

	Temperature (°C)			
	Pt	Rh	Pt + Rh	Pt/Rh
Fresh	254	287	250	252
Thermal aging (40 h)				
700°C, cycled exhaust	289	323	288	246
700°C, air	301	297	304	252
850°C, air	336	450	335	318
Poisoning (35 h)				
450°C, cycled exhaust	257	311	264	260

conversion temperatures during the earlier temperature runup experiments (see Fig. 1). In the absence of a synergism between Pt and Rh, then, the 50% conversion temperature in this feedstream would remain near 280°C regardless of the catalyst composition. In contrast, Fig. 4 shows that the actual 50% conversion temperature goes through a minimum as the Pt content in the catalyst pellet increases, indicating the presence of beneficial Pt–Rh synergisms over the wide catalyst composition range considered. Data for catalysts with Pt contents higher than 83 at.% could not be obtained because of the difficulty associated with preparing such Pt/Rh catalysts that contain both metals in essentially the same band. (Higher Pt loadings tended to make the Pt band substantially wider than the Rh band.) For reference purposes the data for the Pt-only catalyst (0.054 wt% Pt, same data as shown in Fig. 1) are also included in Fig. 4.

Effects of Catalyst Aging

Table 2 shows how the oxidation activity of the Pt, Rh, Pt + Rh, and Pt/Rh (standard bimetallic listed in Table 1) catalysts, as measured by the temperature for 50% CO conversion, is affected by thermal aging and phosphorus poisoning. Here the amounts of the catalyst samples were chosen to give the same number of noble metal atoms (Pt plus Rh if both are present) in all cases. In accordance with earlier observations (*20, 21*), the Pt catalyst suffered substantial losses in oxidation activity after the various thermal treatments, while the phosphorus poisoning had only a small effect on its 50% conversion temperature. It should be noted that the Pt catalyst is somewhat more susceptible to thermal treatment in an oxidizing environment (air, 700°C) than it is in cycled engine exhaust (10 s reducing and 10 s oxidizing, 700°C).

Interestingly, just the opposite trend was found for the Rh catalyst after 700°C treatments; thermal aging in air was observed to be less detrimental than its exposure to the cycled exhaust. Notice, however, that oxidizing treatment at a higher temperature (850°C) severely deactivated the Rh catalyst. This dramatic loss of catalytic activity may be related to harmful interactions between Rh oxide and alumina at elevated temperatures (*22*). It is also evident from Table 2 that Rh is more susceptible than Pt to phosphorus poisoning.

The results for the physical mixture are generally in line with what one would ex-

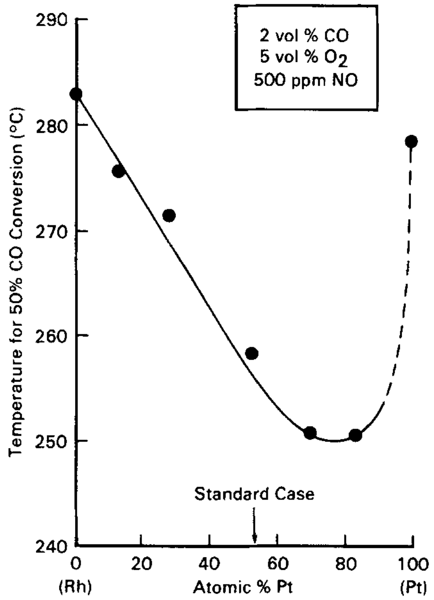

FIG. 4. Temperature for 50% CO conversion for fresh Pt/Rh bimetallic catalysts as a function of catalyst composition. The total number of noble metal atoms in the catalyst sample was held constant.

pect from the activity data of the individual noble metals. Comparisons made between Pt + Rh and Pt/Rh in Table 2 (the same absolute amount of each of the noble metals in both cases) show that the Pt/Rh bimetallic catalyst provided better resistance to thermal aging under various conditions. It is particularly noteworthy that the bimetallic catalyst exhibits remarkable thermal stability with respect to 700°C aging; its 50% conversion temperature remained virtually the same as the fresh value even after 40-h thermal treatments at 700°C, either in air or in cycled exhaust. Although more severe thermal aging (air, 850°C) resulted in substantial deactivation of the bimetallic catalyst, its oxidation activity after the aging still remained significantly higher than that of the physical mixture (nearly 20°C difference in the 50% conversion temperature). Also, the similar 50% conversion temperatures observed for the poisoned physical mixture and bimetallic catalyst indicate that the resistance to phosphorus poisoning is little affected by the difference in the noble metal distribution strategy considered here.

DISCUSSION

To understand the origin of the Pt–Rh synergism, it is useful to discuss the nature of the bimetallic catalyst surface. The Pt/Rh bimetallic catalysts used in this study were prepared using a two-step impregnation procedure (deposition of Rh followed by Pt) with a 2-h 300°C air-calcination step between successive noble metal impregnations. This stepwise impregnation technique (rather than simultaneous impregnation of the two metals) was employed to prepare catalysts with reasonably well-defined surface structure. After the Rh impregnation and subsequent calcination (air, 300°C), the catalyst surface is expected to be populated primarily by Rh_2O_3 (*19*). It is reasonable to assume that during the subsequent Pt impregnation, the noble metal complex (H_2PtCl_6) in acetone solution would display similar affinity for both the alumina support and rhodium oxide. [This argument of similar affinities is supported by the observation that Pt impregnation profiles obtained by the acetone-based technique were not significantly affected by the presence of a variety of base metal oxides on alumina supports (*7*).] In this case, then, the majority of the Pt metals would be deposited onto the alumina surface rather than on top of the rhodium oxide particles because the fraction of the support surface area covered by the rhodium oxide particles is estimated to be quite small. From these considerations, it is reasonable to visualize the surface structure of our bimetallic catalysts as a statistical mixture of Pt and Rh sites that exist on the support surface as separate entities.

Direct experimental verification of the proposed surface structure of the bimetallic catalyst is complicated by the limited ability of most characterization methods to provide structural information on highly dispersed supported catalyst systems. As will become apparent in the following discussion, however, the catalyst surface structure proposed above provides a reasonable basis for rationalizing our observations of synergistic enhancement of CO oxidation activity over the Pt/Rh bimetallic catalyst.

The results of Figs. 2 to 4 illustrate that the Pt–Rh synergism in the bimetallic catalysts leads to improvements in fresh CO oxidation activity over the wide ranges of operating conditions and catalyst composition. To explain this beneficial synergism between Pt and Rh, it is instructive to first examine the adsorptive/catalytic properties of the individual noble metals. It is well established that the primary reaction pathway for CO oxidation on noble metals is a surface reaction between adsorbed CO and adsorbed atomic oxygen (*23*). Over the CO concentration and temperature ranges of interest here, CO oxidation activity over the Pt-only catalyst is generally low because the Pt surface is predominantly covered with CO, leaving very little room for oxygen adsorption [e.g., (*24, 25*)]. Rhodium, on the other hand, readily forms oxides under the net-oxidizing reaction conditions considered in this study (*19*) and this oxide formation has been shown to suppress CO chemisorption significantly (*26*). Consequently, the Rh-only catalyst exhibits relatively low CO oxidation activity under the net-oxidizing conditions, as shown in Fig. 1 (*19, 27*). Low catalytic activity resulting from this insufficiency of one of the key adsorbed reactants (either CO or oxygen) on the catalyst surface would still prevail in the physical mixture of the Pt and Rh catalysts. However, this will no longer be the case for the bimetallic catalyst where Pt (CO source) and Rh (oxygen source) are randomly distributed on the surface; the attendant increase in the probability of finding surface CO and oxygen in the vicinity of each other would lead to higher CO oxidation activity over the bimetallic catalyst.

Another possible interpretation of the Pt–Rh synergism in CO oxidation might be that the platinum enhances the activity of the rhodium by promoting and stabilizing a reduced condition of Rh. [Recall that rhodium metal is more active than its oxide for CO oxidation (*19, 27*).] A similar argument was used to explain enhanced activity of supported nickel oxide catalysts upon addition of platinum or palladium (*28, 29*). One of the characteristics of this NiO activation process was a promoter-like function of the platinum-group metals; the addition of very small amounts of platinum or palladium (in their atomic ratio to nickel as low as 5×10^{-3}) was found to be sufficient for activity enhancement, and larger amounts of the platinum-group metals had little additional effects on the activity of the NiO catalyst (*28, 29*). In contrast, we observed that the CO oxidation activity of the Pt/Rh bimetallic catalysts increased gradually with increasing Pt content up to about 70 at.% Pt (see Fig. 4). Such a gradual increase in activity with increasing Pt tends to argue against the promoter role of the Pt; rather, it suggests that the Pt in the bimetallic catalyst directly participates in the catalytic reaction.

The underlying concept adopted here to explain the improved catalytic activity of the Pt/Rh bimetallic catalyst is of "structural" or "geometrical' nature; the surface structure of the bimetallic catalyst is visualized as a statistical mixture of individual metal sites whose properties are essentially preserved. In addition to such geometrical effects, it is possible that the nearest neighbors to a given metal site may influence its adsorptive properties and hence catalytic behavior as a result of charge transfer from one metal to the other (i.e., "electronic" or "ligand" effects). Unambiguous separation of the contributions of these two effects is generally difficult and is beyond the scope of this work. As can be seen from the above discussion, however, the Pt–Rh synergism observed with our bimetallic catalyst can be rationalized primarily in terms of the geometrical effects.

We made cursory examinations of two questions pertinent to the beneficial Pt–Rh synergism in CO oxidation. First, does simultaneous impregnation of the noble metals (as is commonly used for the preparation of bimetallic catalysts) lead to a similar Pt–Rh synergism? Second, how closely do the Pt and Rh sites need to be in contact in order to have significant synergistic effects?

To address the first question raised above, a new bimetallic catalyst was prepared by simultaneous impregnation of Pt and Rh (acetone technique followed by 500°C air calcination; nominal loadings = 0.05 wt% Pt and 0.03 wt% Rh), and its oxidation activity was compared with that of the standard bimetallic catalyst prepared by the two-step impregnation procedure. Such a comparison is made in Arrhenius plots of the reaction rates shown in Fig. 5. (Here the reactor outlet concentrations were held constant at 1 vol% CO, 5 vol% O_2, and 500 ppm NO during the rate measurements.) It can be seen in Fig. 5 that the simultaneous impregnation of the two noble metals leads to much lower oxidation activity (by a fac-

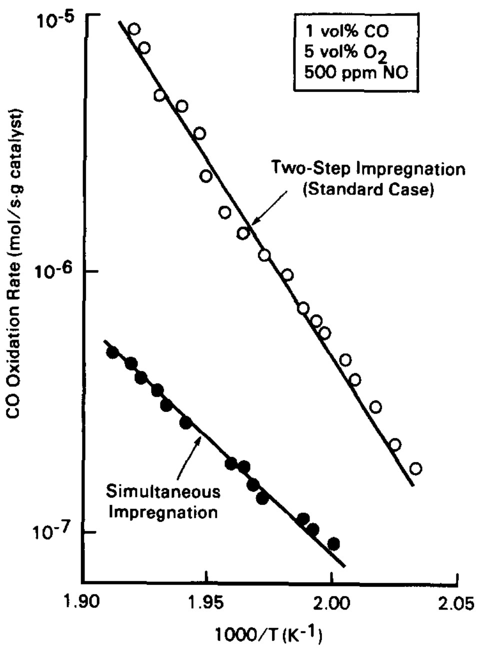

FIG. 5. Arrhenius plots for CO oxidation over the fresh bimetallic catalysts prepared by stepwise and simultaneous impregnation procedures.

tor of 10 or more for T >240°C) than the stepwise impregnation procedure used for the preparation of the standard bimetallic catalyst. This drastic difference in activity appears to be related to a difference in catalyst surface structure between the two types of bimetallic catalysts. When two miscible metals with similar properties (such as Pt and Rh) are codeposited on a support to give a highly dispersed bimetallic catalyst, one might expect on statistical grounds that the individual metal clusters would contain atoms of both metals (i.e., "bimetallic clusters") (*30*). [The formation of Pt–Rh alloys under our oxidizing conditions is ruled out in view of a recent EXAFS study of alumina-supported Pt/Rh catalysts (*31*).] The rate data shown in Fig. 5 imply that the formation of such Pt/Rh bimetallic clusters is undesirable for CO oxidation under oxidizing conditions. This observation can be rationalized as follows.

We postulate that the calcination (air, 500°C, 4 h) after the simultaneous metal impregnation and/or the oxidizing environment used for the activity measurements might have led to segregation of Rh to the surface of the bimetallic clusters. A computational study by Burton *et al.* (*32*) suggests that such surface enrichment [well known for bulk alloys (*33*) and alloy particles (*34*)] can also occur in highly dispersed bimetallic microclusters through the segregation of one component to the surface sites having low coordination numbers, such as corners and edges. Liao *et al.* (*35*) used hydrogen chemisorption and XPS to characterize alimina-supported Pt/Cu catalysts and found preferential Cu enrichment to the surface of the bimetallic catalysts. Our XPS studies of a Pt/Rh sample (2 wt% Pt/1 wt% Rh simultaneously impregnated on ground alumina) showed similar surface enrichment in Rh after air calcination at 500°C; the Rh-to-Pt surface atomic ratio was found to be nearly 3 compared to the bulk atomic ratio of 1. Additional evidence for Rh enrichment of the bimetallic clusters was obtained by measurements of CO oxidation activity as a function of inlet CO concentration. The results of such experiments are shown in Fig. 6, together with the activity data for the 0.026 wt% Rh catalyst (same data shown in Fig. 1). The striking similarity between the two curves in their concentration dependence of CO oxidation activity is a strong indication that the bimetallic catalyst prepared by simultaneous impregnation behaves Rh-like, lending further support to our hypothesis of surface Rh enrichment in the bimetallic clusters. This Rh-enriched surface, as a result of its tendency to form a relatively inactive Rh oxide in an oxidizing environment, resulted in poorer CO oxidation activity than the standard Pt/Rh bimetallic catalyst, as demonstrated in Fig. 5.

Regarding the intimacy requirement for the synergism, the absence of significant synergistic effects for the physical mixture of the Pt and Rh catalyst pellets (3.5 mm diam) rules out the possibility of interaction via long-lived species in the gas phase. To

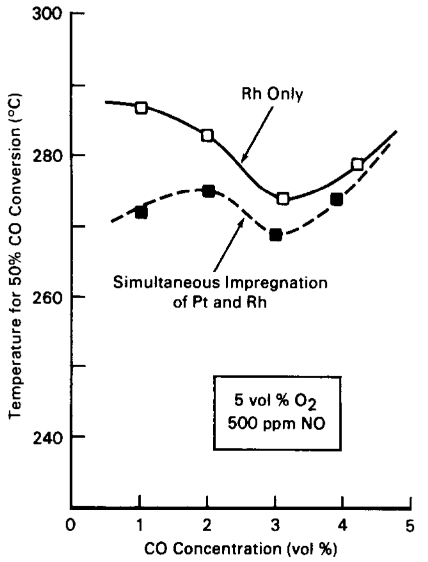

FIG. 6. Comparison of the dependence of CO oxidation activity on inlet CO concentration level for the Rh catalyst and the Pt/Rh bimetallic catalyst prepared by simultaneous impregnation of the noble metals.

see if more intimate physical contact between the metal particles induces the Pt–Rh synergism, rate measurements were performed with a sample prepared by thoroughly grinding together appropriate amounts of the two single-component catalysts (about one-half of the powder in a size range of <100 μm). The ground mixture was pressure-pelletized into self-supporting disks each 2 cm in diameter and ~200 μm thick. It was found that these pressed pellets did not exhibit synergistic activity enhancement as was observed for the standard bimetallic catalyst. This suggests the possibility that short-range surface interactions between the platinum and rhodium particles may be needed for the synergism.

Recall that all the catalysts discussed above were calcined (air, 500°C, 4 h) after final metal impregnation. To examine the catalytic effect of reducing treatments, the standard bimetallic catalyst (which had already been air-calcined) was treated in H_2 at 500°C for 5 h. Subsequent activity measurements showed that this additional hydrogen treatment temporarily enhanced the CO oxidation activity of the Pt/Rh bimetallic catalyst (presumably due to the high activity of the reduced Rh) but did not change its stabilized activity. This is not surprising because the supported Rh surface is expected to equilibrate readily with its oxidizing gaseous environment used during the activity measurements, regardless of the nature of heat treatment after catalyst preparation (*19*).

To assess the importance of impregnation sequence and solvent to the Pt–Rh synergism, we also briefly examined two additional bimetallic catalysts prepared by stepwise impregnation: one using the reverse sequence of impregnations (Fig. 7B) and the other using acetone as the impregnating solvent for both metal deposition steps (Fig. 7C). Although these two bimetallic catalysts exhibited some deviations in the apparent activation energy and reaction rate from the standard bimetallic catalyst (Fig. 7A), the curves for the three cases are all clustered reasonably closely at an activ-

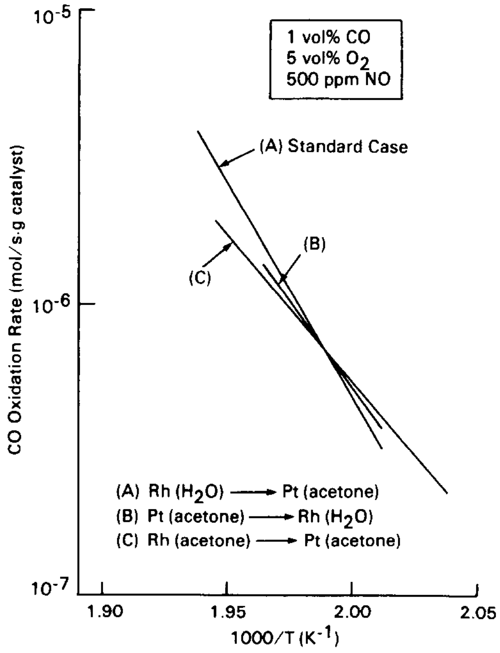

FIG. 7. Arrhenius plots for CO oxidation over the fresh bimetallic catalysts prepared by three different stepwise impregnation procedures.

ity level substantially higher than that of the bimetallic catalyst prepared by simultaneous impregnation (compare Figs. 5 and 7). This demonstrates the generality of our conclusion that stepwise impregnation of Pt and Rh leads to higher CO oxidation activity than simultaneous metal impregnation.

Regarding the effect of thermal aging on CO oxidation activity (see Table 2), the observation of better thermal stability of Rh than Pt after the 700°C oxidizing treatment is consistent with the order of stability toward crystallite growth predicted by Wynblatt and Gjostein (*36*). After being treated in air at 850°C, however, the ranking was reversed; the Rh catalyst requires a much higher temperature for 50% CO conversion than the Pt catalyst. This reversal of ranking cannot be rationalized based on the relative rates of Pt and Rh crystallite growth; this observation strongly suggests that other mechanisms, such as the metal–support interaction proposed by Yao *et al.* (*22*), are also responsible for the deactivation of the Rh catalyst in this high-temperature oxidizing environment. The mechanism whereby multicomponent supported catalysts sinter has received little attention in the literature. It is beyond the scope of this work to ascertain the reasons for the good thermal stability of our Pt/Rh bimetallic catalyst (see Table 2). Nevertheless, it is reasonable to consider the possibility that the separation of the Pt particles by the more thermally stable Rh particles on the surface of the bimetallic catalyst may have improved its sintering characteristics by retarding the rate of surface migration of Pt. Several recent sintering studies (*37—39*) have reported similar enhancement of the thermal stability of supported catalysts by addition of a second metal.

In addition to CO oxidation activity discussed above, the selectivity for promoting the CO–NO reaction versus the CO–O_2 reaction at warmed-up converter temperatures is an important factor in exhaust emission control applications. (Of course, high selectivity for the CO–NO reaction is desired.) Selectivity measurements at 450°C showed rather small differences in the selectivity among the fresh Rh, Pt + Rh, and Pt/Rh catalysts. This indicates that Rh is primarily responsible for the CO–NO reaction, with Pt playing only a minor role as a result of its limited ability to dissociate molecularly adsorbed NO (*40*). After thermal aging (850°C, air, 40 h), however, the bimetallic catalyst exhibited substantially higher selectivity for NO conversion than the physical mixture. Further work is required to understand this sintering-induced selectivity changes.

CONCLUDING REMARKS

Our laboratory reactor experiments have shown that over the range of CO and O_2 concentrations encountered during the converter warmup period, the Pt/Rh bimetallic catalyst prepared by stepwise metal impregnation exhibits substantially higher CO oxidation activity than the physical mixture of the Pt and Rh catalysts containing the same absolute amount of each of the noble metals. This activity enhancement due to the Pt–Rh synergism can be rationalized by visualizing the surface structure of the bimetallic catalyst as a random mixture of Pt and Rh sites. Furthermore, the superiority of the bimetallic catalyst to the physical mixture was found to carry over to CO oxidation activity after high-temperature catalyst aging in either air or cycled engine exhaust.

This beneficial synergistic effect was not observed over the Pt/Rh bimetallic catalyst prepared by simultaneous impregnation of the two noble metals, a method commonly used for the preparation of bimetallic catalysts. This preparative procedure leads to the enrichment of the catalyst surface with relatively inactive rhodium oxides under net-oxidizing reaction conditions, resulting in poor CO oxidation activity.

The results of this study demonstrate the importance of understanding interactions between the noble metals (with respect to catalytic activity and durability) in the development of improved automotive catalysts. In addition, catalyst preparation procedures (e.g., simultaneous vs stepwise impregnation) can have profound effects on the catalyst surface structure and thus on the catalytic properties of the resulting bimetallic catalyst, as illustrated here for Pt/Rh three-way catalysts.

Extrapolation of our results to the actual exhaust environment, of course, should be done with caution in view of the simple laboratory feedstreams and accelerated catalyst aging schedules employed in this study. Furthermore, commercial three-way catalysts usually contain significant amounts of base metal additives such as CeO_2. In addition to the Pt/Rh interactions discussed here, the interactions between the base metal additives and the noble metals can play an important role in determining the performance and durability characteristics of three-way automotive catalysts. The latter aspects await future study.

ACKNOWLEDGMENTS

The authors gratefully acknowledge R. A. Waldo and A. Ottolini, both of the Analytical Chemistry Department, for providing the XPS and electron microprobe data. Engine dynamometer aging of the catalysts was done by R. W. Richmond and D. J. Upton of the Physical Chemistry Department.

REFERENCES

1. Jacobson, R. L., Kluksdahl, H. E., McCoy, C. S., and Davis, R. W., *Proc. Amer. Petrol. Inst., Div. of Refin.* **49,** 504 (1969).
2. Pollitzer, E. L., *Platinum Met. Rev.* **16** (2), 42 (1972).
3. Burch, R., *Platinum Met. Rev.* **22** (2), 57 (1978).
4. Carter, J. L., McVicker, G. B., Weissman, W., Kmak, W. S., and Sinfelt, J. H., *Appl. Catal.* **3,** 327 (1982).
5. Sinfelt, J. H., and Via, G. H., *J. Catal.* **56,** 1 (1979).
6. Wagstaff, N., and Prins, R., *J. Catal.* **59,** 446 (1979).
7. D'Aniello, M. J., Jr., U.S. Patent 4,380,510, April 19, 1983.
8. Cavanagh, R. R., and Yates, J. T., Jr., *J. Chem. Phys.* **74,** 4150 (1981).
9. Yates, D. J. C., Murrell, L. L., and Prestridge, E. B., *J. Catal.* **57,** 41 (1979).
10. Worley, S. D., Rice, C. A., Mattson, G. A., Curtis, C. W., Guin, J. A., and Tarrer, A. R., *J. Chem. Phys.* **76,** 20 (1982).
11. Yao, H. C., and Rothschild, W. G., *J. Chem. Phys.* **68,** 4774 (1978).
12. Taylor, K. C., and Schlatter, J. C., *J. Catal.* **63,** 53 (1980).
13. Dictor, R. A., personal communications, General Motors Research Laboratories, Warren, Mich., 1985.
14. Via, G. H., Meitzner, G., Lytle, F. W., and Sinfelt, J. H., *J. Chem. Phys.* **79,** 1527 (1983).
15. Hegedus, L. L., and Baron, K., *J. Catal.* **54,** 115 (1978).
16. Berty, J. M., *Chem. Eng. Prog.* **70,** 78 (1974).
17. Voltz, S., Morgan, C., Liederman, D., and Jacob, S., *Ind. Eng. Chem. Prod. Res. Dev.* **12,** 294 (1973).
18. Kim, Y., Shi, S.-K., and White, J. M., *J. Catal.* **61,** 374 (1980).
19. Oh, S. H., and Carpenter, J. E., *J. Catal.* **80,** 472 (1983).
20. Klimisch, R. L., Summers, J. C., and Schlatter, J. C., *Adv. Chem. Ser.* **143,** 103 (1975).
21. Hegedus, L. L., and Summers, J. C., *J. Catal.* **48,** 345 (1977).
22. Yao, H. C., Japar, S., and Shelef, M., *J. Catal.* **50,** 407 (1977).
23. Engel, T., and Ertl, G., *Adv. Catal.* **28,** 1 (1979).
24. McCarthy, E., Zahradnik, J., Kuczynski, G. C., and Carberry, J. J., *J. Catal.* **39,** 29 (1975).
25. Schlatter, J. C., and Chou, T.-S., "Measuring CO Oxidation Rates in a Recycle Reactor," presented at the AIChE 71st Annual Meeting, Miami Beach, November 1978.
26. Zhu, Y., and Schmidt, L. D., *Surf. Sci.* **129,** 107 (1983).
27. Kiss, J. T., and Gonzalez, R. D., *J. Phys. Chem.* **88,** 898 (1984).
28. Nowak, E. J., and Koros, R. M., *J. Catal.* **7,** 50 (1967).
29. Charcosset, H., Frety, R., Soldat, A., and Trambonze, Y., *J. Catal.* **22,** 204 (1971).
30. Sinfelt, J. H., *Prog. Solid State Chem.* **10,** 55 (1975).
31. Broach, R. W., Hickey, J. P., and Lester, G. R., "EXAFS Study of Oxidized and Reduced Platinum–Rhodium on Gamma Alumina Catalysts," presented at the ACS Annual Meeting, Washington, D.C., August 1983.
32. Burton, J. J., Hyman, E., and Fedak, D. G., *J. Catal.* **37,** 106 (1975).
33. Williams, F. L., and Nelson, G. C., *Appl. Surf. Sci.* **3,** 409 (1979).
34. Wang. T., and Schmidt, L. D., *J. Catal.* **71,** 411 (1981).

35. Liao, P. C., Carberry, J. J., Fleisch, T. H., and Wolf, E. E., *J. Catal.* **74,** 307 (1982).
36. Wynblatt, P., and Gjostein, N. A., *Prog. Solid State Chem.* **9,** 21 (1975).
37. McVicker, G. B., Garten, R. L., and Baker, R. T. K., *J. Catal.* **54,** 129 (1978).
38. Zhdan, P. A., Kuznetsov, B. N., Shepelin, A. P., Kovalchuk, V. I., and Yermakov, Y. I., *React. Kinet. Catal. Lett.* **18,** 267 (1981).
39. Bartholomew, C. H., Pannell, R. B., and Fowler, R. W., *J. Catal.* **79,** 34 (1983).
40. Root, T. W., Schmidt, L. D., and Fisher, G. B., *Surf. Sci.* **134,** 30 (1983).